Ion size effects on the osmotic pressure and electrocapillarity in a nanoslit: Symmetric and asymmetric ion sizes

Rajni,[1] J. M. Oh,[1,2,*] and I. S. Kang[1,†]

[1]*Department of Chemical Engineering, Pohang University of Science and Technology, 77 Cheongam-Ro, Nam-Gu, Pohang, Gyeongbuk, 37673, Republic of Korea*

[2]*Center for Soft and Living Matter, Institute for Basic Science (IBS), 50 UNIST-gil, Ulju-gun 44919, Republic of Korea*

(Received 10 March 2016; revised manuscript received 18 May 2016; published 20 June 2016)

We analyze the effect of asymmetric finite ion size in nanoconfinement in the view of osmotic pressure and electrocapillarity. When the confinement width becomes comparable with the Debye length, the overlapped electric double layer is significantly deformed by the steric effects. We derive the osmotic pressure from the modified Poisson-Boltzmann equation in a nanoslit to examine the deviation from the ideal osmotic pressure and the repulsive force on the wall considering the asymmetry of ion sizes. Then the electrocapillarity due to the steric effect is investigated under constant potential condition with the flat interface assumption. Later, the deformation by the electrocapillarity is also considered in the first order approximation.

DOI: 10.1103/PhysRevE.93.063112

I. INTRODUCTION

Nanoslit walls immersed in an electrolyte solution attract counterions to exhibit the electrocapillarity phenomenon. The electrocapillary phenomenon refers to the modification of the interfacial tension by the presence of electrical charges in multiphase flows. Electrocapillarity is also referred to as the single phase flows through capillaries in the presence of an electric double layer (EDL) as studied by Ghosal [1], which is out of scope in the present work. The first investigation on this phenomenon was performed by Lippman in 1875 [2]. Many theoretical works have been performed on the electrocapillary phenomena based on the well-known Lippmann equation [3], which was originally developed for a perfectly conducting fluid such as mercury. Several efforts have been made to extend this theory [4]. There are basically two different approaches: the free-energy based approach and the electromechanical approach. Buehrle *et al.* [5] used the free-energy based approach to extend the theory to an electrolyte system. Biesheuvel [6] obtained electrostatic free energy considering chemical work together with electrical work. On the other hand, Jones [7] and Kang [8] used the electromechanical approach to derive the Lippmann equation. Kang *et al.* [9] extended the theory for an aqueous electrolyte system with a finite thickness of electrical double layer. Hua *et al.* [10] extended it further to incorporate the steric effect of ions. The electrocapillarity of an electrolyte in a nanoslit with overlapped EDL was investigated by Lee and Kang [11] based on the Poisson-Boltzmann equation. Electrocapillarity or electrowetting has been regarded as an efficient tool for handling microfluidics [12,13]. It has been applied to various areas in nanofluidics and optofluidics [14].

When the length scale gets smaller down to the nanoscale of $O(10\ \text{nm})$ comparable with the Debye length, the continuum approach is still valid, but the physics may not be the same as in the bulk [15,16]. In a nanoslit, the overlapped EDL is formed and the coions are excluded at some level from the nanoslit. The electrolyte is subjected to two different kinds of interactions, known as van der Waals interactions and electric double layer (EDL) electrostatic interactions. These interactions operate on different length scales. The EDL electrostatic interactions are quantified by the osmotic pressure. The osmotic pressure plays a major role in many significant physiochemical process such as the swelling of microcapsules [17,18]. Therefore the EDL electrostatic interaction formed near the interface is of utmost importance in many applications such as electrochemistry, electrophoresis, and nanofluidics [19]. The classical Poisson-Boltzmann (PB) equation describes the EDL potential, from which the osmotic pressure can be derived. But this theory fails in explaining various electrokinetic phenomena at nanometer length scales as the size of the ions becomes comparable to the nanoslit widths. Thus it becomes extremely important to incorporate the size of ions in the modeling of the system at such length scales.

In many cases, it is common to assume the ionic species as point charges neglecting the effect of their sizes even when the EDL overlap is considered. However, the finite volume of the ions can have tremendous influence on various applications of nanoscale electrokinetic phenomena [20–30]. Apart from steric effects, a couple of researchers have also studied the effects of dielectric polarization at nanoscale separations [31,32]. The confinement effect has been investigated for a long time by many researchers. Stern introduced the corrections to the Poisson-Boltzmann equations and indicated the volume constraints of ions in the electrolyte phase [33]. Bikerman developed the first complete ion-size-effect-induced modified Poisson-Boltzmann model [34]. Since then, Bikerman's modified Poisson-Boltzmann equation (MPB) was reformulated by Eigen and Wicke [35,36], Strating and Wiegel [37,38], Borukhov *et al.* [39], and Bohinc and coresearchers [40,41]. Kilic *et al.* [42] applied the same equation for the analysis of the concentrated electrolytes. Trizac and Raimbault [43] studied long-range electrostatic interactions between like-charged colloids taking into account steric and confinement effects. Kornyshev derived a model equation including the steric effect in a statistical mechanics way based on the concept of Fermi distribution concerning the consequences on the diffuse layer capacitances [44]. Bazant *et al.* [29]

*jmo0902@gmail.com
†iskang@postech.ac.kr

reviewed the modified Poisson-Boltzmann equations taking into consideration steric effects. They extended Bikerman's equation to include the electrostatic correlation effect (or overscreening effect). However, most of these studies deal with the symmetric size of cations and anions. There are a few studies incorporating the asymmetric ion sizes, too, by Georgi *et al.* [45], Popović and Šiber [46], Zhou *et al.* [47], Li [48], Li *et al.* [49], and Han *et al.* [50].

The steric effects in the confinement have gotten attention because of their importance. Das and Chakraborty [51] investigated the steric effect leading to a significant enhancement in the EDL overlap. Moon *et al.* [52] investigated especially the effects of correlation length on osmotic pressure. However, even though studies have been carried out to understand EDL structure, there is still a lack of systematic understanding of the effect of finite asymmetric ion size on the osmotic pressure and electrocapillarity of an electrolyte in a nanoslit.

In this paper, the modified Poisson-Boltzmann equation proposed by Han *et al.* [50] is solved to investigate the steric effects of ions on the osmotic pressure and electrocapillarity in a nanoslit with respect to symmetric and asymmetric size of ions. The effect of electrocapillarity is represented as the sum of the osmotic pressure and the Maxwell stress contribution. Thus the steric effects on the osmotic pressure are investigated first. The analysis of osmotic pressure helps us to calculate the repulsive force exerted on the walls of the nanoslit as it is known that the repulsive force per unit of slit wall area is the same as the osmotic pressure at the nanoslit centerline [11,53]. The repulsive force on the nanoslit wall occupies a very important position in many applications [17,18,54–56]; thus osmotic pressure at the slit centerline attracts special attention in this investigation. After calculation of osmotic pressure, the Maxwell stress is obtained and added to the osmotic pressure contribution to obtain the total normal stress exerted on the gas-electrolyte interface. The average value of this total normal stress is regarded as the measure of the electrocapillarity effect.

II. GOVERNING EQUATIONS AND METHODS

A. Modeling of steric effect of ions in an electrolyte

In this section, the model equations for electric potential of electrolytes confined in a nanoslit with a given zeta potential are briefly reviewed. Then, in the next section, the osmotic pressure change due to the electric potential is derived. We consider electrolytes confined in a nanoslit as shown in Fig. 1. The sizes of cation and anion may be different (symmetric or asymmetric) and the thickness of the nanoslit ($2h$) is comparable with Debye length (κ^{-1}). An electric potential V is applied at the nanoslit wall ($x = \pm h$).

We will adapt the recent work of Han *et al.* [50] who studied the mean field theory (MFT) on the differential capacitance of asymmetric ionic liquid electrolytes. The derivation starts with the Helmholtz free energy of the system, i.e.,

$$F = e\phi(N_+ - N_-) - k_B T \ln\Omega, \tag{1}$$

where N_+ and N_- denote the number of cations and anions, respectively. ϕ and e are the electrostatic potential and the elementary electron charge, respectively. The second term on the right-hand side of Eq. (1) represents the entropic

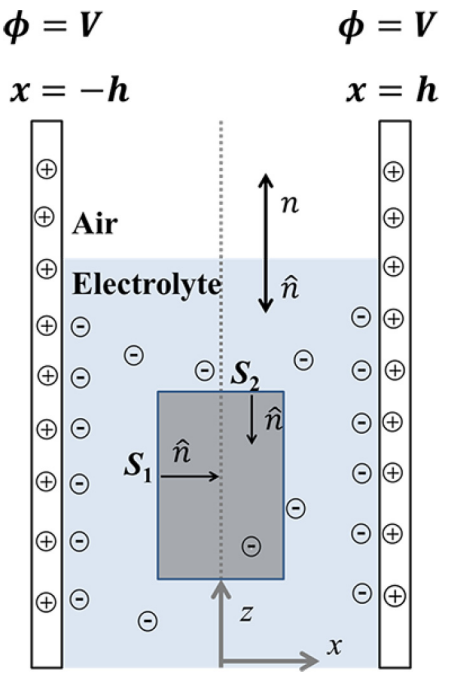

FIG. 1. Electrolyte confined in a nanoslit with the surface potential V at the walls.

contribution to the free energy, where k_B is the Boltzmann constant, T is the temperature, and Ω is the number of possible distributions of ions. In this model, the correlation between the ions is neglected. To take into account asymmetric sized ions, a new parameter ξ is introduced for the volume ratio of an anion to a cation, i.e.,

$$\xi = \frac{V_-}{V_+} = \frac{a_-^3}{a_+^3}, \tag{2}$$

where a_+ and a_- represent the radii of cation and anion, respectively. Here we assume that the size of the anion is less than or equal to that of the cation ($\xi \leqslant 1$). Note that a large asymmetry means a small value of ξ.

The steric effect parameter γ is also defined as $\gamma = 2n_b a_i^3$, where $a_i = a_+$ is the radius of a cation or $a_i = a_-$ is the radius of an anion. Thus the dimensionless modified Poisson-Boltzmann equation becomes (see the detailed derivation in Appendix)

$$\tilde{\nabla}^2 u = -\frac{1}{\gamma}\frac{\exp(-u) - \exp(u)\left[\frac{\xi\exp(u)+\eta}{\xi+\eta}\right]^{(1/\xi)-1}}{\exp(-u) + (\xi+\eta)\left[\frac{\xi\exp(u)+\eta}{\xi+\eta}\right]^{1/\xi}}, \tag{3}$$

where $\tilde{\nabla}^2 = \partial^2/\partial X^2$. The length scale for nondimensionalization is chosen as the Debye length ($X = \kappa x$), and the dimensionless potential is set as $u = \frac{ze\phi}{k_B T}$. The compressibility γ and porosity η are defined as follows:

$$\gamma = \frac{2N_0}{N} \quad \text{and} \quad \eta = \frac{2}{\gamma} - 1 - \xi$$

When $\xi = 1$, Eq. (3) reduces to the modified Poisson-Boltzmann equation for symmetric ion sizes.

B. Osmotic pressure in a nanoslit expressed in terms of electric field

Let us briefly remind the reader of osmotic pressure in nanoconfinement. When there is no fluid flow with negligible gravity, the total stress is described as the sum of the osmotic pressure contribution and the Maxwell stress contribution, which can be expressed as

$$\mathbf{T} = -\pi\mathbf{I} + \mathbf{T}^e = -\pi\mathbf{I} + \varepsilon\varepsilon_0\left[\mathbf{EE} - \tfrac{1}{2}E^2\mathbf{I}\right]. \quad (4)$$

Here $\pi(x)$ is the osmotic pressure which is a function of the position vector. In the case of a nanoslit, it is assumed that the electric field has only the x component, i.e.,

$$\mathbf{E} = E\mathbf{e}_x = E(x)\mathbf{e}_x. \quad (5)$$

Let us now consider the shaded region in Fig. 1. Then on the surface S_1, which is parallel to the nanoslit centerline; T_{xx} is the inward normal stress. Thus the outward normal stress $(-T_{xx})$ acts like the pressure exerted on the surface. Let us denote it by P_{xx}. Then,

$$P_{xx} \equiv -T_{xx} = \pi(x) - \frac{\varepsilon\varepsilon_0}{2}[E(x)]^2. \quad (6)$$

The osmotic pressure $\pi(x)$ can be obtained from the relation [10,11,43]

$$\nabla\pi = \rho_f\mathbf{E}, \quad (7)$$

where ρ_f is the free charge density given as $\rho_f = \varepsilon\varepsilon_0\nabla\cdot\mathbf{E}$. By solving Eq. (7) for a one-dimensional (1D) problem, we have

$$\pi(x) = \frac{\varepsilon\varepsilon_0}{2}[E(x)]^2 + \pi(0), \quad (8)$$

where $\pi(0)$ is the osmotic pressure at the slit centerline. Substituting this into Eq. (6), we have

$$P_{xx} \equiv -T_{xx} = \pi(0) = \text{constant with respect to } x. \quad (9)$$

The total outward normal stress on the plane S_1 is constant across the nanoslit width and it is equal to the osmotic pressure at the centerline. Therefore $\pi(0)$ is the repulsive force per unit area of the slit wall [11,53].

C. Electrocapillarity in terms of electric field

Let us now consider the surface S_2, which is perpendicular to the nanoslit centerline, shown in Fig. 1. The outward normal stress exerted on S_2 is given as

$$P_{zz} \equiv -T_{zz} = \pi(x) - \frac{\varepsilon\varepsilon_0}{2}[E(x)]^2. \quad (10)$$

Note the sign change in the Maxwell stress contribution on comparing the above equation with Eq. (6), which implies that the P_{ij} field is anisotropic [11,43]. The outward normal stress exerted on the surface perpendicular to the slit centerline is not uniform across the slit width. This nonuniform distribution of P_{zz} leads to the deformation of the interface [11]. When we consider the osmotic pressure relative to the bulk osmotic pressure, $\Delta\pi(x) = \pi(x) - \pi_b$, the outward normal stress represents pure electrical effect. Let us denote it by P^e_{zz}. The average value of P^e_{zz} can be regarded as the measure of the electrocapillarity effect.

$$\overline{P^e_{zz}} = \frac{1}{h}\int_0^h P^e_{zz}(x)dx = \Delta\pi(0) + \frac{\varepsilon\varepsilon_0}{h}\int_0^h [E(x)]^2 dx. \quad (11)$$

From Eq. (11), we can see that $\overline{P^e_{zz}} \geqslant \pi(0)$, always. This means that the electrocapillarity is always larger than the repulsive force exerted on a unit area of the slit wall.

III. STERIC EFFECTS ON THE OSMOTIC PRESSURE

The potential distribution is obtained numerically for asymmetrical ionic sizes and it is used to obtain the osmotic pressure. The osmotic pressure can be obtained by integrating $\nabla\pi = \rho_f\mathrm{E}$, which is $\nabla\pi = -(k_BT/ze)\rho_f(u)\nabla u$ in terms of u. By using the free charge density formula and the condition $\pi = \pi_b$ when $u = 0$, we have the osmotic pressure for the asymmetrical ionic sizes in a nanoslit as

$$\Delta\pi(X) = \frac{2n_bk_BT}{\gamma}\left[\ln\left\{\exp(-u) + (\xi+\eta)\left[\frac{\xi\exp(u)+\eta}{\xi+\eta}\right]^{1/\xi}\right\} + \ln\left\{\frac{\gamma}{2}\right\}\right]. \quad (12)$$

Equation (12) denotes the deviation from bulk pressure and solely represents the confinement effect. Similarly with the modified Poisson-Boltzmann equation, when $\xi = 1$, Eq. (12) reduces to the osmotic pressure for symmetric ion sizes,

$$\Delta\pi(X) = \pi(X) - \pi_b = \frac{2n_bk_BT}{\gamma}\ln[1+\gamma(\cosh(u)-1)]. \quad (13)$$

For the case of symmetric ion sizes, the ion distributions are governed by

$$n_\pm = \frac{n_be^{\mp u}}{1+\gamma[\cosh(u)-1]}. \quad (14)$$

In Eq. (13), π_b is the osmotic pressure in the bulk where the electric potential is assumed to be zero. Here it should be noted that π_b may be different from $2n_bk_BT$ because of the steric effect of ions. In fact, it is given as [56]

$$\pi_b = -2n_bk_BT\frac{\ln(1-\gamma)}{\gamma}. \quad (15)$$

The π_b is a monotonically increasing function and reaches near $4n_bk_BT$ at $\gamma = 0.8$, which implies that even ideal bulk pressure increases significantly due to steric effect. The same formula has been rederived recently by the free-energy approach [30].

A. Deviation from ideality

Some conclusions may be drawn without detailed computation results. From Eq. (13), we observe that the osmotic pressure decreases monotonically as the steric effect increases at fixed electric potential, i.e.,

$$\left[\frac{\partial(\Delta\pi)}{\partial\gamma}\right]_\phi < 0. \quad (16)$$

In the high electric potential limit (i.e., $\phi\to\infty$), we have simpler limiting forms. If there is no steric effect ($\gamma = 0$),

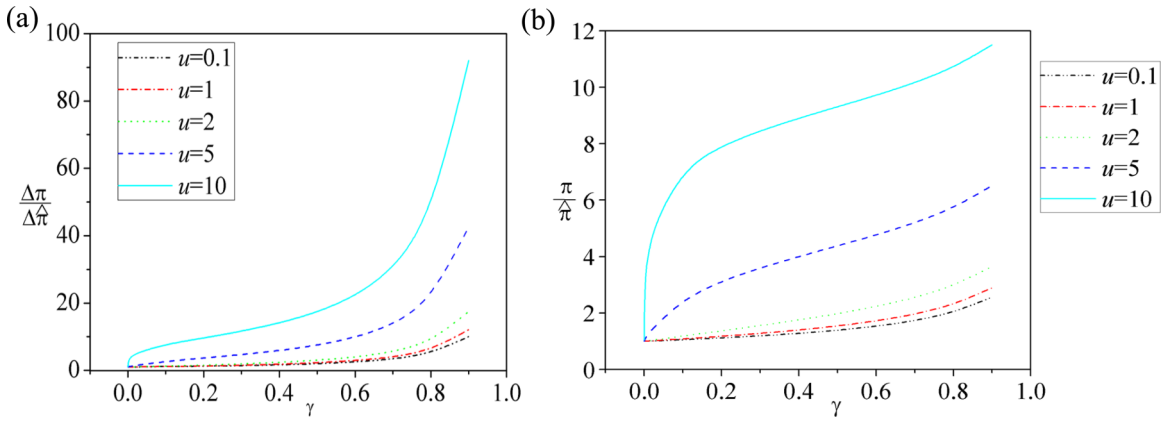

FIG. 2. Steric effects on deviation from the ideal solution from the viewpoint of (a) osmotic pressure difference and (b) the osmotic pressure [$\pi = \Delta\pi + \pi_b$ and $\hat{\pi} = (n_+ + n_-)k_BT$].

we have $\Delta\pi \to 2n_b k_B T \cosh(\phi/V_T)$ and if the steric effect is finite, we have $\Delta\pi \to 2n_b(ze\phi)/\gamma$. It is noteworthy that the osmotic pressure increases linearly with the electric potential in the case of finite steric effect, while it increases exponentially in the case of no steric effect [10]. Another point is that the osmotic pressure is inversely proportional to the steric effect parameter in the high electric potential limit if the potential is held constant.

In the result of Eq. (13), two counteracting effects are combined. The total number of ions decreases due to the steric effect according to the formula (14) when the electric potential is fixed. But for the same number densities of ions, the steric effect increases the osmotic pressure. In order to represent the latter effect, we define the osmotic pressure increase $\Delta\hat{\pi}(x)$, that is the osmotic pressure increase of the corresponding ideal solution with the same number densities, as

$$\Delta\hat{\pi}(x) = (n_+ + n_- - 2n_b)k_BT. \tag{17}$$

In Eq. (17), the number densities n_+ and n_- are determined according to Eq. (14). When the steric effect is small ($0 < \gamma \ll 1$), the ratio of the osmotic pressure to that of the ideal solution for the same ion number densities is

$$\frac{\Delta\pi}{\Delta\hat{\pi}} = \frac{2n_b}{(n_+ + n_- - 2n_b)\gamma} \times \left(\ln\left\{ \exp(-u) + (\xi+\eta)\left[\frac{\xi\exp(u)+\eta}{\xi+\eta}\right]^{1/\xi} \right\} + \ln\left(\frac{\gamma}{2}\right) \right) = 1 + \frac{\gamma}{2}\left(\frac{n_+ + n_-}{2n_b} + 1\right) + \cdots. \tag{18}$$

Equation (18) shows that the steric effect increases the osmotic pressure at the same number densities.

In Fig. 2(a), the numerically computed ratio $\Delta\pi/\Delta\hat{\pi}$, which represents the dimensionless deviation from ideality, is plotted against the steric effect parameter γ. For the given dimensionless potential u, the ion concentrations are the same for both cases and determined by Eq. (14), but Eq. (13) is used for the computation of $\Delta\pi$, while Eq. (17) is used for $\Delta\hat{\pi}$. The deviation from the ideality of the solution becomes very large (more than 50 times larger than the ideal solution in $\gamma > 0.8$) as the dimensionless potential increases. It is also notable that $\Delta\pi/\Delta\hat{\pi}$ can be more than 5 even for $\gamma < 0.2$. And, when u is high enough (for example, $u = 10$), there is a steep increase of $\Delta\pi/\Delta\hat{\pi}$ in $\gamma < 0.05$. From this result, we can see that the steric effect may increase significantly the osmotic pressure when the number densities are fixed. However, from Eq. (16), the osmotic pressure $\Delta\pi$ decreases with respect to the steric effect at fixed electric potential. This means that the decrease of the total number density due to the steric effect is so large [see Eq. (14)] that the osmotic pressure decreases as a whole even though the osmotic pressure increases for the same number densities as shown in Fig. 2(a). In Fig. 2(b), the ratio of the osmotic pressures $\pi/\hat{\pi}$ is plotted against steric parameter γ, where $\pi = \Delta\pi + \pi_b$ and $\hat{\pi} = (n_+ + n_-)k_BT$ with the bulk osmotic pressure given by Eq. (15). So the bulk pressure π_b is included in both π and $\hat{\pi}$, whose effect softens the deviation from ideality. As shown in Fig. 2(b), $\pi/\hat{\pi}$ increases monotonically, but its slope is not so steep in $0.2 < \gamma < 0.8$ compared with $\Delta\pi/\Delta\hat{\pi}$.

B. Steric effects on the repulsive force on the wall

As mentioned earlier, the repulsive force on the unit area of the nanoslit wall is equal to the osmotic pressure at the centerline, i.e., $\Delta\pi(0)$. In Fig. 3, the dimensionless repulsive force $\Delta\pi(0)$ (with respect to the counteracting bulk osmotic pressure contribution) is shown as a function of the steric parameter γ for two values of the nanoslit width at various surface potentials where $V_s = V/V_T$, where V_T is the thermal voltage. For $\kappa h = 2$, the repulsive force, which is maximized at $\gamma = 1$, increases monotonically with the steric effect parameter in $V_s = 2{-}6$. However, in the case of moderate to high potentials ($V_s = 7{-}10$), the repulsive force is maximized in $\gamma < 1$, and the critical γ for the maximum decreases gradually with respect to V_s. This nonmonotonous behavior of the repulsive force is due to a combined effect: decrease of number density and increase of osmotic pressure with respect to γ, which is mentioned in the previous section. Due to the small width of the nanoslit, the maximum is obtained after which the osmotic pressure decreases. It means the osmotic pressure on the wall can be maximized at a certain volume

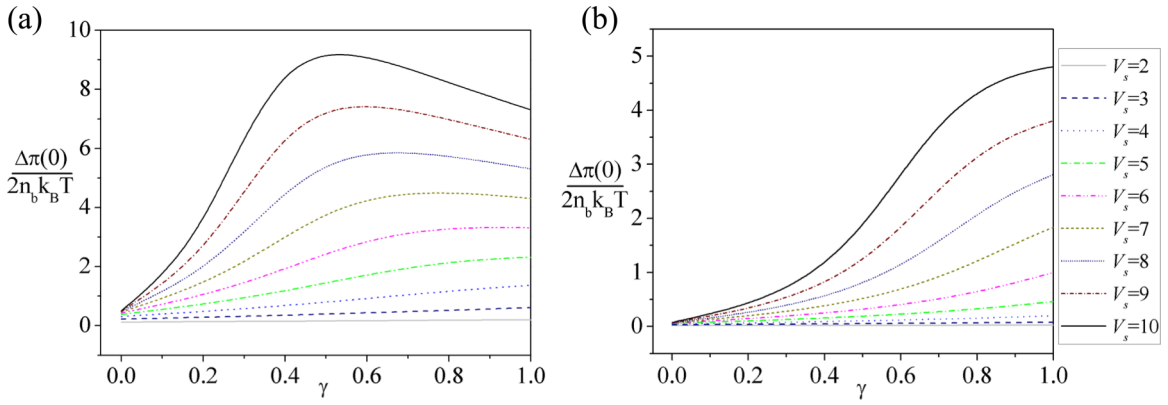

FIG. 3. Osmotic pressure at the nanoslit centerline for symmetric size of ions for (a) $\kappa h = 2$ and (b) $\kappa h = 3$ at various surface potentials where $V_s = V/V_T$.

fraction of charge at high potential. If the slit width is large enough ($\kappa h = 3$), the nonmonotonous behavior disappears.

Previously we have shown that the osmotic pressure difference $\Delta\pi$ decreases with the steric effect if the electric potential is fixed. However, we must note that the electric potential at the centerline increases with the steric effect as shown in Fig. 4. Since the influence of the increased electric potential is larger than the decreasing effect of γ for a fixed electric potential, the repulsive force increases monotonically with the steric effect parameter as shown in Fig. 3 for the case of $\kappa h = 2,3$. This phenomenon may be explained in physical terms as follows. When the steric effect parameter increases, the total number of ions that can be accommodated in the nanoslit decreases. Therefore the total number of counterions also decreases due to the increased steric effect. This means that the shielding effect of ions decreases and the electric potential at the centerline increases as shown in Fig. 4.

Figure 5 shows the steric effect dependence on the osmotic pressure at the center for various slit widths. As the width of the nanoslit increases the maximum osmotic pressure shifts towards the right and decreases in magnitude as shown in Fig. 5. As the nanoslit width increases, the EDL overlapping phenomenon decreases. Thus decreasing potential at the nanoslit center reduces the osmotic pressure and the surface potential at which the maximum starts to occur increases.

The present model is compared with the previous work by Lee and Kang [11], which does not consider the steric effect. Figure 6 compares the osmotic pressures at the channel center with respect to slit width κh for $V_s = 1$ and 10 with $\gamma = 0.1$. The plot can be divided into three regions: small ($\kappa h < 1$), middle ($1 < \kappa h < 3$), and wider ($3 < \kappa h$) ranges. For the small range, the steric effect becomes significant to induce substantially higher osmotic pressure even for a small steric factor ($\gamma = 0.1$). In the middle range of κh, the osmotic pressure becomes lower than that without steric effect. It is notable that the osmotic pressure with steric effect becomes the same as that without steric effect at $\kappa h = 1$. As the channel width becomes large enough, the steric effect does not play a significant role anymore. This tendency is consistent with $V_s = 1$ and 10, though the deviation is more distinctive at a higher wall potential.

The effect of asymmetry of ionic size is shown in Fig. 7. When the asymmetry parameter ξ decreases, the size of the anions (counterions) gets smaller and more ions can be attracted towards the nanoslit wall. The positively charged nanoslit wall is packed and shielded well by the anions. This results in lower electric potential at the nanoslit centerline and thus the osmotic pressure at the nanoslit centerline decreases. This behavior is similar to that in the case of symmetric ion sizes. With the increase in nanoslit width the osmotic

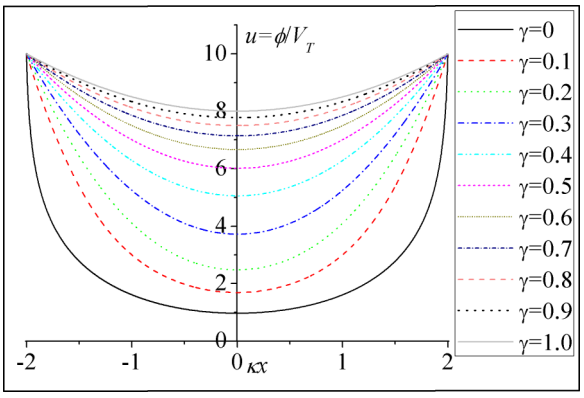

FIG. 4. The steric effect of ions on the electric potential distribution. The EDL overlapping is more pronounced as the steric effect increases.

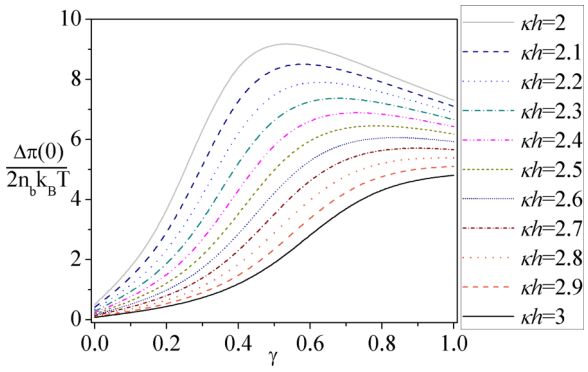

FIG. 5. Variation of osmotic pressure at the nanoslit centerline at $V_s = 10$ with respect to steric factor as nanoslit width increases from $\kappa h = 2$ to $\kappa h = 3$.

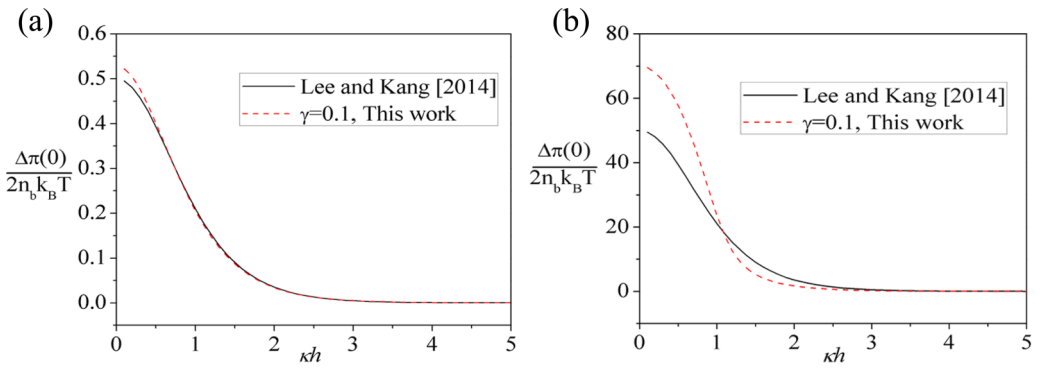

FIG. 6. The comparison of osmotic pressures at the channel center with respect to slit width κh for $V_s = 1$ and 10 with $\gamma = 0.1$.

pressure at the nanoslit centerline decreases. Therefore, as the asymmetry of the ions increases (with smaller ξ), the repulsive force on the nanoslit wall decreases. In other words, if you want to have a higher osmotic pressure in a nanoslit, it is preferable to use an electrolyte with similar sizes of anions and cations.

IV. STERIC EFFECTS ON THE ELECTROCAPILLARITY

A. Steric effects on the electrocapillarity under the constant potential condition at the slit wall

In this section, we analyze the steric effects on the electrocapillarity at the electrolyte-gas interface using a similar method to that in Lee and Kang [11]. The interface in electrocapillarity is not perfectly flat since the electric field on the interface is not uniform along the interface, which will be discussed later in this section. A couple of studies showed that the interface deformation can be significant and might induce capillary filling in a nanochannel [57–59]. However, we limit our attention only to the flat interface in order to treat the problem analytically as we did in our previous work [11]. We are mainly interested in the pure steric effects on the electrocapillarity and focus on the averaged normal stress over the interface. We will also consider the interface deformation with the first order approximation later in this section. It is assumed that the electric permittivity of the electrolyte is much larger than that of the gas; i.e., $\varepsilon \gg \varepsilon_{\text{out}}$. Then the component of the electric field normal to the interface vanishes and the assumption that $\mathbf{E} = E(x)\mathbf{e}_x$ is valid in a nanoslit up to the flat interface. Due to the absence of osmotic pressure in the gas phase and since the electric permittivity of the gas phase is much smaller than that of the electrolyte, the normal stress due to the electric field in the gas phase can be neglected compared to the electrolyte. The outward normal stress on the electrolyte-gas interface results in the capillary rise in the nanoslit.

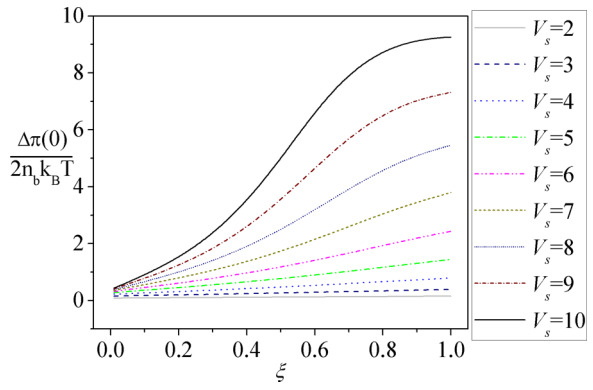

FIG. 7. The effect of asymmetric behavior of ionic size on the osmotic pressure at the nanoslit centerline for different surface potentials at fixed steric factor of $\gamma = 0.5$ and $\kappa h = 2$.

The formula for the averaged outward normal stress (with respect to the osmotic pressure in the bulk), i.e., $\overline{P^e_{zz}}$, was given earlier in Eq. (11). By choosing V_T, κ^{-1}, and $(2n_b k_B T)$ as the characteristic voltage, the length scale, and the characteristic stress scale respectively, we define the dimensionless potential and coordinate as $u = \phi/V_T$ and $X = \kappa x$. Then by substituting $E(x) = -\frac{d\phi}{dx} = -\kappa V_T \frac{du}{dX}$ into Eq. (11) and by Eq. (12) of the osmotic pressure, and with the help of $\kappa^2 = (2n_b z^2 e^2/\varepsilon\varepsilon_0 k_B T)$, we have the dimensionless averaged outward normal stress $\overline{P_{zz}}^* = \overline{P^e_{zz}}/(2n_b k_B T)$ as

$$\begin{aligned}\overline{P_{zz}}^* &= \frac{1}{2n_b k_B T}\left\{\Delta\pi(0) + \frac{\varepsilon\varepsilon_0}{h}\int_0^h [E(x)]^2 dx\right\} \\ &= \frac{1}{\gamma}\left(\ln\left\{\exp(-u) + (\xi+\eta)\left[\frac{\xi\exp(u)+\eta}{\xi+\eta}\right]^{1/\xi}\right\}\right. \\ &\quad \left. + \ln\left(\frac{\gamma}{2}\right)\right) + \frac{1}{\kappa h}\int_0^{\kappa h}\left(\frac{du}{dX}\right)^2 dX. \end{aligned} \tag{19}$$

When $\xi = 1$, Eq. (19) reduces to the dimensionless averaged outward normal stress equation for symmetric ion sizes.

$$\overline{P_{zz}}^* = \frac{1}{\gamma}\ln\{1+\gamma[\cosh(u)-1]\} + \frac{1}{\kappa h}\int_0^{\kappa h}\left(\frac{du}{dX}\right)^2 dX. \tag{20}$$

From the above, we can see that the electrocapillarity consists of two contributions. The first is the osmotic pressure at the slit centerline (which is the same as the repulsive pressure exerted on the slit wall) and the second is the electrical stress contribution. The osmotic pressure depends on the electric potential at the slit centerline while the electrical stress depends on the gradient of the electric potential across the slit. If we look at the electric potential distribution in Fig. 4,

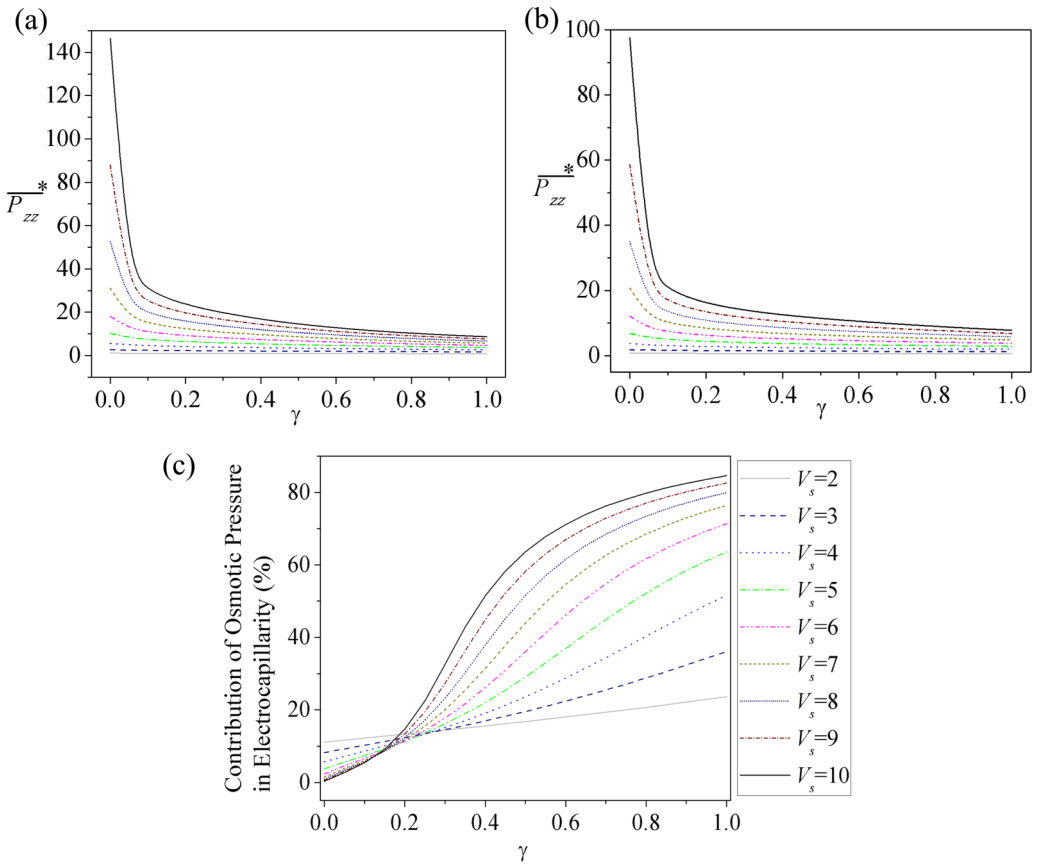

FIG. 8. Total outward normal stress on the interface of the electrolyte in the nanoslit for symmetric sizes of ions for (a) $\kappa h = 2$, (b) $\kappa h = 3$, and (c) contribution of osmotic pressure in electrocapillarity with $\kappa h = 2$ at various surface potentials.

the centerline value increases as the steric factor increases. Therefore the repulsive pressure on the wall increases as we have discussed in the previous section. On the other hand, the magnitude of the gradient decreases and the second term decreases as the steric factor increases. Since the effect of the second term is larger than the first term, as a whole the electrocapillarity effect decreases as the steric factor increases as seen in Fig. 8. The decreasing effect is more pronounced for larger values of the slit wall potential and the smaller slit gap size. A similar tendency was found for the steric effect on the wetting tension in charge related macroscale wetting phenomena [10].

When the ions have asymmetric sizes, then the electrocapillarity effect increases as the size of the anion (counterion) decreases as shown in Fig. 9. This tendency is again similar to that of the symmetric size of ions.

When the asymmetric behavior of ions is considered, the anions have smaller sizes and the nanoslit wall potential considered in the problem is positive. But if the nanoslit wall has negative potential, then the osmotic pressure is almost constant with respect to the change in size of the coions as shown in Fig. 10. In the negative surface potential case, the anions are the coions. When ξ decreases (asymmetry of ion size increases), the size of the anions (coions) is smaller and cations, being bulky, limit the ions attracted to the nanoslit wall. The repulsion between the bulky cation and the nanoslit wall provides space for the smaller anions, which leads to better shielding.

B. Steric effects on electrocapillarity at the constant charge condition

In reality, the nanoslit walls in most cases can be described by the constant charge conditions. The results for the constant voltage conditions can be converted to those for constant charge conditions without much difficulty by using the relation $-\varepsilon\varepsilon_0(\frac{\partial\phi}{\partial x}) = |\sigma_w|$, where σ_w is the surface charge density. However, compared to the cases of no steric effects, we have a special point to be considered. Due to the finite size of the ions, the number of ions in the nanoslit would be limited and the

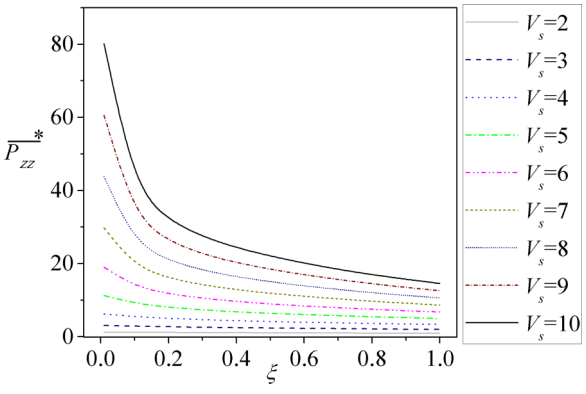

FIG. 9. The total outward normal stress exerted on the interface of the electrolyte in the nanoslit for asymmetric sizes of ions for nanoslit width $\kappa h = 2$ at steric factor $\gamma = 0.5$ for various surface potentials.

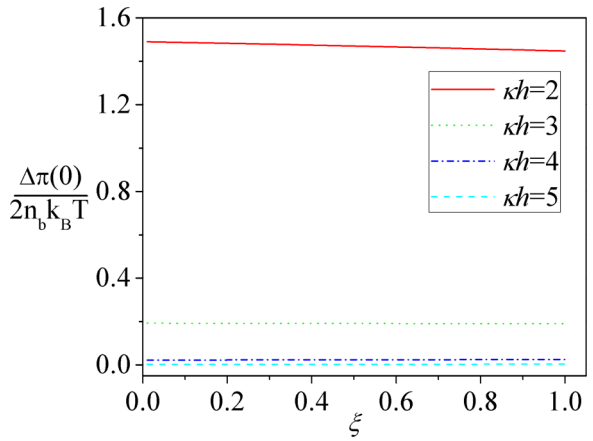

FIG. 10. The effect of asymmetric ionic sizes on the osmotic pressure at the nanoslit centerline for different nanoslit widths at surface potential $V_s = -5$.

charge neutrality condition limits the allowable surface charge density. It may induce interesting problems for the constant charge conditions. However, in this paper, a further study will not be conducted due to the length of the paper.

C. Deformation of the electrolyte-gas interface due to steric effect

Here we predict the deformation of the electrolyte-gas interface due to the nonuniform normal stress with a first order approximation. The analysis scheme is similar to the previous work of Lee and Kang [11]. When some potential is applied, the normal stress deforms the interface into a certain shape. This deformation is determined by the normal stress condition,

$$\mathbf{n}\cdot(\mathbf{n}\cdot\mathbf{T}_{\text{out}}) - \mathbf{n}\cdot(\mathbf{n}\cdot\mathbf{T}_{\text{in}}) = \gamma_s \nabla\cdot\mathbf{n}, \tag{21}$$

with $\mathbf{T}_{\text{out}} = -P^h_{\text{out}}\mathbf{I}$ and $\mathbf{T}_{\text{in}} = -\pi\mathbf{I} + \mathbf{T}^e - P^h_{\text{in}}\mathbf{I}$, where the superscript h denotes the hydrostatic pressure and γ_s is the surface tension of the electrolyte-gas interface. Thus with the help of Eq. (10) we have, for the initially flat interface,

$$-T^e_{nn} + \pi - \left(P^h_{\text{out}} - P^h_{\text{in}}\right) = P_{zz} - \left(P^h_{\text{out}} - P^h_{\text{in}}\right) = \gamma_s \nabla\cdot\mathbf{n}. \tag{22}$$

We adopt the domain perturbation technique to solve this problem under the assumption that the deformation from the initial shape is small and that the electric field deviation due to the interface deformation is negligible. The shape function of the interface is introduced as

$$F(x,z) = z - f(x) = 0. \tag{23}$$

Then the curvature is approximated in the first order accuracy as

$$\nabla\cdot\mathbf{n} = \frac{\partial n_x}{\partial x} + \frac{\partial n_z}{\partial z} \simeq -f''. \tag{24}$$

Substituting Eq. (24) into Eq. (22), we obtain the governing equation for the first order deformation as follows:

$$f'' = -\frac{1}{\gamma_s}\left[P_{zz} - \left(P^h_{\text{out}} - P^h_{\text{in}}\right)\right] \equiv -\frac{1}{\gamma_s}\left[P_{zz} - \Delta P^h\right]. \tag{25}$$

In our study, the focus is on the osmotic pressure and electrocapillarity that leads to deformation of the interface. Thus for simplicity, we consider only the case of an initially flat interface with a fixed contact angle with $f'(h) = 0$ at the wall. In addition, we set $f(0) = 0$ as a reference point of deformation. The unknown value of the pressure difference $\Delta P^h = (P^h_{\text{out}} - P^h_{\text{in}})$ is determined so as to satisfy the boundary condition $f'(h) = 0$. Thus we have (for the details, see Lee and Kang [11])

$$\Delta P = \frac{1}{h}\int_0^h P_{zz}\,dx = \overline{P_{zz}}. \tag{26}$$

By substituting the expressions of P_{zz} and $\overline{P_{zz}}$ from Eqs. (10) and (11) into Eq. (26), we have

$$f'' = -\frac{1}{\gamma_s}[P_{zz} - \overline{P_{zz}}] = \frac{\varepsilon\varepsilon_0}{\gamma_s}\left\{\frac{1}{h}\int_0^h [E(x)]^2 dx - [E(x)]^2\right\}. \tag{27}$$

Since $E = -\nabla\phi = -\kappa V_T \frac{du}{dX}$, we have the following governing equation for the dimensionless shape function $f^* = f/h$:

$$\frac{d^2 f^*}{dX^2} = \frac{\text{Ca}_\pi}{(\kappa h)^2}\left[\frac{1}{\kappa h}\int_0^{\kappa h}\left(\frac{du}{dX}\right)^2 dX - \left(\frac{du}{dX}\right)^2\right], \tag{28}$$

with the boundary conditions $f^*(0) = 0$ and $\frac{df^*}{dX}(\kappa h) = 0$. In Eq. (28), Ca_π is the capillary number based on the thermal voltage defined as $\text{Ca}_\pi = \frac{1}{\gamma_s}(\varepsilon\varepsilon_0\kappa^2 V_T^2 h)$.

Figure 11 shows the dimensionless interface deformation for various γ and V_s for a nanoslit width $\kappa h = 2$. The interface

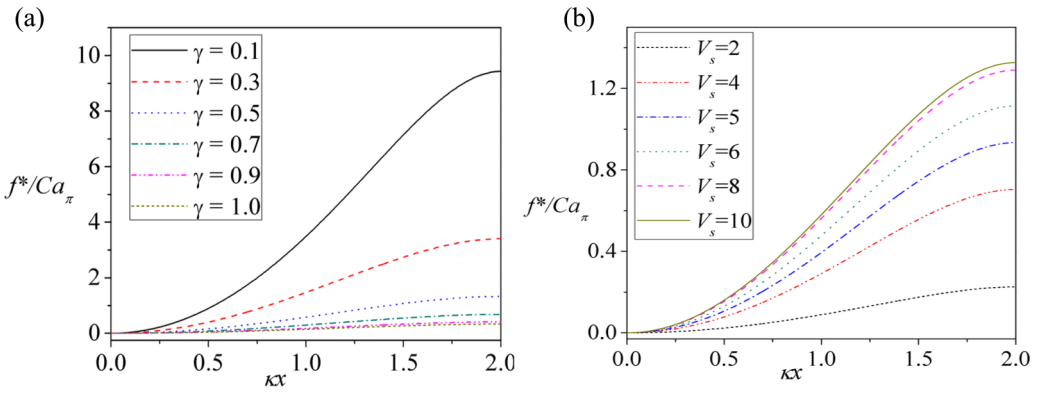

FIG. 11. Steric effect on the interface deformation under the fixed contact angle condition for $\kappa h = 2$ with respect to (a) γ and (b) V_s.

is pushed to the air side near the wall. It is interesting to find that the overall degree of deformation decreases with respect to γ [Fig. 11(a)]. The deformation f^* can be larger than 5 times the capillary number Ca_π for low γ, but it becomes smaller than Ca_π for higher γ. It implies that the flat interface assumption can be verified for higher γ, whose case is the main concern in this paper. However, for fixed γ, the deformation becomes large with higher V_s, as expected intuitively, as shown in Fig. 11(b). The deformation pattern is similar at both low and high surface potentials.

V. CONCLUSIONS

The modified Poisson-Boltzmann equation is used to study the steric effects on the osmotic pressure and the electrocapillarity in a nanoslit. Since the osmotic pressure at the slit centerline is equal to the repulsive force exerted on the unit area of the slit wall, special attention is given to it [11,53]. The electrocapillarity is evaluated in the form of the average value of the outward total normal stress exerted on the electrolyte-gas interface.

The steric effect on the osmotic pressure is analyzed under the condition of fixed electric potential at the slit walls. It has been known from a previous work that the steric effect reduces the osmotic pressure at a certain point if the electric potential is fixed [10]. However, along the nanoslit centerline, the situation is more complicated than expected because the electric potential changes with the steric effect parameter. The electric potential increases as the steric effect increases due to smaller shielding effect. Thus the two effects play roles in opposite directions. However, as a whole the osmotic pressure at the slit centerline (or the repulsive force on the wall) increases with the increase of the steric parameter when the slit width is larger than a certain value. If the slit width is smaller than the value, the osmotic pressure at the centerline increases initially, but decreases after the maximum value for larger values of the steric parameter. The osmotic pressure increases with respect to surface potentials. The osmotic pressure obtained by the current model is compared with the results of Lee and Kang [11]. The outward normal stress at the electrolyte-gas interface $\overline{P^e_{zz}}$ strongly depends on the square of the electric field strength in the electric double layer [Eq. (11)]. Thus the electrocapillarity decreases as the steric effect increases because the EDL overlapping increases with the increase of the steric parameter.

However, in the case of asymmetric ion sizes, the size of the counterion turns out to be important. The size of the coion does not have significant effects. As the size of the counterion increases, the degree of EDL overlapping increases and the osmotic pressure at the nanoslit centerline also increases. On the other hand, the electrocapillarity decreases with the increase of the size of the counterion. Thus as the asymmetry of the ions decreases, the osmotic pressure increases and electrocapillarity decreases.

ACKNOWLEDGMENTS

This research at POSTECH was supported by the Basic Science Research Program through the National Research Foundation of Korea (NRF) funded by the Ministry of Science, ICT, and Future Planning (Grant No. 2013R1A1A2011956) and BK21 program of Korea. The research at IBS Center for Soft and Living Matter was supported by the Institute for Basic Science (Project Code No. IBS-R020-D1).

APPENDIX: DERIVATION OF THE MODIFIED POISSON-BOLTZMANN EQUATION FOR ASYMMETRIC ION SIZES

We will adapt the recent work of Han *et al.* [50] who studied the mean field theory (MFT) on the differential capacitance of asymmetric ionic liquid electrolytes. To obtain the possible distributions of ions, Ω, i.e., $\Omega = \Omega_+\Omega_-$. Denoting the total number of available lattices by N, those occupied by cations are $\Omega_+ = N!/N_+!(N-N_+)!$. Thus the number of lattices left for the anions is $[(N-N_+/\xi)]$ and $\Omega_- = [(N-N_+/\xi)]/N_-!\{[(N-N_+/\xi)]-N_-\}!$. Thus

$$\Omega = \frac{N!}{N_+!(N-N_+)!}\frac{[(N-N_+/\xi)]!}{N_-!\{[(N-N_+/\xi)]-N_-\}!}. \quad \text{(A1)}$$

Using the Stirling approximation, i.e.,

$$\ln N! \approx N\ln N - N \quad \text{for} \quad N \gg 1, \quad \text{(A2)}$$

we have

$$\ln\Omega = N\ln N - N_+\ln N_+ - (N-N_+)\ln(N-N_+) - N_-\ln N_- + \tfrac{N-N_+}{\xi}\ln\tfrac{N-N_+}{\xi} - (\tfrac{N-N_+}{\xi}-N_-)\ln(\tfrac{N-N_+}{\xi}-N_-).$$

Minimizing the free energy with respect to N_+ and N_-, we have the chemical potential as

$$\mu_+ = \frac{\partial F}{\partial N_+} = e\phi - k_BT\left[\ln(N-N_+) - \ln N_+ + \frac{1}{\xi}\ln\left(\frac{N-N_+}{\xi}-N_-\right) - \frac{1}{\xi}\ln\left(\frac{N-N_+}{\xi}\right)\right], \quad \text{(A3)}$$

$$\mu_- = \frac{\partial F}{\partial N_-} = -e\phi - k_BT\left[\ln\left(\frac{N-N_+}{\xi}-N_-\right) - \ln N_-\right]. \quad \text{(A4)}$$

Equalizing the chemical potential of each kind of ion at a given potential to that of the bulk of the electrolyte where $\phi = 0$ and $N_+ = N_- = N_0$, we have

$$e\phi - k_BT\left[\ln\frac{N-N_+}{N-N_0} - \ln\frac{N_+}{N_0} + \frac{1}{\xi}\ln\frac{N-N_+-\xi N_-}{N-N_0-\xi N_0} - \frac{1}{\xi}\ln\frac{N-N_+}{N-N_0}\right] = 0, \quad \text{(A5)}$$

$$-e\phi - k_BT\left[\ln\frac{N-N_+-\xi N_-}{N-N_0-\xi N_0} - \ln\frac{N_-}{N_0}\right] = 0. \quad \text{(A6)}$$

Rewriting the above equations in terms of ionic concentration, and denoting the average ionic concentration in the bulk of the electrolyte as n_b, the potential-dependent ionic

concentration, n_+ and n_-, may be written as [50]

$$\frac{n_+}{n_b} = \frac{N_+}{N_0} = \frac{2}{\gamma}\frac{\exp(-u)}{\exp(-u) + (\xi+\eta)\left[\frac{\xi\exp(u)+\eta}{\xi+\eta}\right]^{1/\xi}}, \quad \text{(A7)}$$

$$\frac{n_-}{n_b} = \frac{N_-}{N_0} = \frac{2}{\gamma}\frac{\exp(-u)\left[\frac{\xi\exp(u)+\eta}{\xi+\eta}\right]^{(1/\xi)-1}}{\exp(-u) + (\xi+\eta)\left[\frac{\xi\exp(u)+\eta}{\xi+\eta}\right]^{1/\xi}}, \quad \text{(A8)}$$

where the dimensionless potential $u = \frac{ze\phi}{k_B T}$ and compressibility γ and porosity η are defined as

$$\gamma = \frac{2N_0}{N} \quad \text{and} \quad \eta = \frac{2}{\gamma} - 1 - \xi. \quad \text{(A9)}$$

With the ionic concentration n_b known, the potential-dependent charge density distribution may be written as

$$\rho(u) = e(n_+ - n_-) = \frac{2en_b}{\gamma}\frac{\exp(-u) - \exp(u)\left[\frac{\xi\exp(u)+\eta}{\xi+\eta}\right]^{(1/\xi)-1}}{\exp(-u) + (\xi+\eta)\left[\frac{\xi\exp(u)+\eta}{\xi+\eta}\right]^{1/\xi}}. \quad \text{(A10)}$$

When $\xi = 1$, the ions have the same size and the expression becomes the Kornyshev equation [44]:

$$\rho(u) = -2en_b\frac{\sinh(u)}{1 + 2\gamma\sinh^2(u/2)}. \quad \text{(A11)}$$

When $\gamma = 0$, the expression reduces to the Gouy-Chapman model:

$$\rho(u) = -2en_b\sinh(u). \quad \text{(A12)}$$

Thus the dimensionless modified Poisson-Boltzmann equation becomes

$$\tilde{\nabla}^2 u = -\frac{1}{\gamma}\frac{\exp(-u) - \exp(u)\left[\frac{\xi\exp(u)+\eta}{\xi+\eta}\right]^{(1/\xi)-1}}{\exp(-u) + (\xi+\eta)\left[\frac{\xi\exp(u)+\eta}{\xi+\eta}\right]^{1/\xi}}, \quad \text{(A13)}$$

where $\tilde{\nabla}^2 = \partial^2/\partial X^2$ and the length scale is nondimensionalized by the Debye length ($X = \kappa x$). When $\xi = 1$, Eq. (A13) reduces to the modified Poisson-Boltzmann equation for symmetric ion sizes.

[1] S. Ghosal, Annu. Rev. Fluid Mech. **38**, 309 (2006).
[2] J. Newman and K. E. Thomas-Alyea, *Electrochemical Systems*, 3rd ed. (Wiley, New York, 2003).
[3] S. W. J. Smith, Phil. Trans. R. Soc. Lond. A **193**, 47 (1900).
[4] D. C. Grahame and R. B. Whitney, J. Am. Chem. Soc. **64**, 1548 (1942).
[5] J. Buehrle, S. Herminghaus, and F. Mugele, Phys. Rev. Lett. **91**, 086101 (2003).
[6] P. M. Biesheuvel, J. Colloid Interface Sci. **275**, 514 (2004).
[7] T. B. Jones, Langmuir **18**, 4437 (2002).
[8] K. H. Kang, Langmuir **18**, 10318 (2002).
[9] K. H. Kang, I. S. Kang, and C. M. Lee, Langmuir **19**, 5407 (2003).
[10] C. K. Hua, I. S. Kang, K. H. Kang, and H. A. Stone, Phys. Rev. E **81**, 036314 (2010).
[11] J. A. Lee and I. S. Kang, Phys. Rev. E **90**, 032401 (2014).
[12] A. R. Wheeler, Science **322**, 539 (2008).
[13] L. Yeo and H.-C. Chang, Electrowetting, in *Encyclopedia of Microfluidics and Nanofluidics*, edited by D. Li (Springer, New York, 2008), p. 600.
[14] D. Mattia and Y. Gogotsi, Microfluid. Nanofluid. **5**, 289 (2008).
[15] F. Baldessari, J. Colloid Interface Sci. **325**, 526 (2008).
[16] S. Chakraborty, Electrocapillary, in *Encyclopedia of Microfluidics and Nanofluidics*, edited by D. Li (Springer, New York, 2008), pp. 460–469.
[17] K. Köhler, P. M. Biesheuvel, R. Weinkamer, H. Möhwald, and G. B. Sukhorukov, Phys. Rev. Lett. **97**, 188301 (2006).
[18] F. Zhou, P. M. Biesheuvel, E.-Y. Choi, W. Shu, R. Poetes, U. Steiner, and W. T. S. Huck, Nano Lett. **8**, 725 (2008).
[19] M. Tagliazucchi and I. Szleifer, Mater. Today **18**, 131 (2015).
[20] A. Garai and S. Chakraborty, Electrophoresis **31**, 843 (2010).
[21] H. Zhao, J. Phys. Chem. C **114**, 8389 (2010).
[22] A. S. Khair and T. M. Squires, J. Fluid Mech. **640**, 343 (2009).
[23] B. D. Storey, L. R. Edwards, M. S. Kilic, and M. Z. Bazant, Phys. Rev. E **77**, 036317 (2008).
[24] S. Chanda and S. Das, Phys. Rev. E **89**, 012307 (2014).
[25] S. Das, Phys. Rev. E **85**, 012502 (2012).
[26] Y. Liu, M. Liu, W. M. Lau, and J. Yang, Langmuir **24**, 2884 (2008).
[27] M. Z. Bazant, M. S. Kilic, B. D. Storey, and A. Ajdari, Adv. Colloid Interface Sci. **152**, 48 (2009).
[28] M. Z. Bazant, M. S. Kilic, B. D. Storey, and A. Ajdari, New J. Phys. **11**, 075016 (2009).
[29] M. Z. Bazant, B. D. Storey, and A. A. Kornyshev, Phys. Rev. Lett. **106**, 046102 (2011).
[30] J. Andrews and S. Das, RSC Adv. **5**, 46873 (2015).
[31] A. Bandopadhyay, V. A. Shaik, and S. Chakraborty, Phys. Rev. E **91**, 042307 (2015).
[32] R. F. Stout and A. S. Khair, Phys. Rev. E **92**, 032305 (2015).
[33] O. Stern, Z. Elektrochem. **30**, 508 (1924).
[34] J. J. Bikerman, Philos. Mag. **33**, 384 (1942).
[35] M. Eigen and E. Wicke, Naturwissenschaften **38**, 453 (1951).
[36] M. Eigen and E. Wicke, J. Phys. Chem. **58**, 702 (1954).
[37] P. Strating and F. W. Wiegel, J. Phys. A **26**, 3383 (1993).
[38] P. Strating and F. W. Wiegel, Physica A **193**, 413 (1993).
[39] I. Borukhov, D. Andelman, and H. Orland, Phys. Rev. Lett. **79**, 435 (1997).
[40] K. Bohinc, A. Iglič, T. Slivnik, and V. Kralj-Iglič, Bioelectrochemistry **57**, 73 (2002).
[41] K. Bohinc, V. Kralj-Iglič, and A. Iglič, Electrochim. Acta **46**, 3033 (2001).
[42] M. S. Kilic, M. Z. Bazant, and A. Ajdari, Phys. Rev. E **75**, 021502 (2007).
[43] E. Trizac and J.-L. Raimbault, Phys. Rev. E **60**, 6530 (1999).
[44] A. A. Kornyshev, J. Phys. Chem. B **111**, 5545 (2007).
[45] N. Georgi, A. A. Kornyshev, and M. V. Fedorov, J. Electroanal. Chem. **649**, 261 (2010).
[46] M. Popović and A. Šiber, Phys. Rev. E **88**, 022302 (2013).
[47] S. Zhou, Z. Wang, and B. Li, Phys. Rev. E **84**, 021901 (2011).
[48] B. Li, Nonlinearity **22**, 811 (2009).
[49] B. Li, P. Liu, Z. Xu, and S. Zhou, Nonlinearity **26**, 2899 (2013).

[50] Y. Han, S. Huang, and T. Yan, J. Phys.: Condens. Matter **26**, 284103 (2014).
[51] S. Das and S. Chakraborty, Phys. Rev. E **84**, 012501 (2011).
[52] G. J. Moon, M. M. Ahn, and I. S. Kang, Phys. Rev. E **92**, 063020 (2015).
[53] J. N. Israelachvili, *Intermolecular and Surface Forces*, 3rd ed. (Academic Press, New York, 2011).
[54] P. M. Biesheuvel, T. Mauser, G. B. Sukhorukov, and H. Möhwald, Macromolecules **39**, 8480 (2006).
[55] M. J. Park, I. Choi, J. Hong, and O. Kim, J. Appl. Polym. Sci. **129**, 2363 (2013).
[56] D. Ben-Yaakov, D. Andelman, D. Harries, and R. Podgornik, J. Phys. Chem. B **113**, 6001 (2009).
[57] J. Haneveld, N. R. Tas, N. Brunets, H. V. Jansen, and M. Elwenspoek, J. Appl. Phys. **104**, 014309 (2008).
[58] A. Bandopadhyay, S. Mandal, and S. Chakraborty, Soft Matter **12**, 2056 (2016).
[59] A. Dörr and S. Hardt, Phys. Rev. E **86**, 022601 (2012).